Thin Solid Films 556 (2014) 294–299

Contents lists available at ScienceDirect

Thin Solid Films

journal homepage: www.elsevier.com/locate/tsf

The formation of interfacial wrinkles at the metal contacts on organic thin films

Jian-Jhih Fang [a], Huai-Wen Tsai [a], I-Chi Ni [b], Shien-Der Tzeng [b], Mei-Hsin Chen [a,*]

[a] Department of Opto-Electronic Engineering, National Dong Hwa University, Hualien 974, Taiwan
[b] Department of Physics, National Dong Hwa University, Hualien 974, Taiwan

ARTICLE INFO

Article history:
Received 26 September 2013
Received in revised form 8 January 2014
Accepted 15 January 2014
Available online 22 January 2014

Keywords:
Organic photovoltaics
Interfaces
Morphology
Compressive strain

ABSTRACT

The basic mechanism leading to the morphology change in the active layer was explored systematically. We found that the wrinkles appearing at the cathode surface under post-annealing processes are more prominent than those under pre-annealing processes, which is strongly related to the roughness increase of the active layer. Due to thermal-induced instability from the aluminum (Al) layer with the device under post-annealing processes, a net compressive strain develops from the thermal expansion mismatch between the layers. Furthermore, an analysis of the mechanical properties shows that the enlarged nano-dimension roughness of the active layer is dominated by the final-bottom morphology of the compressed Al layer which depends on the annealing sequence.

1. Introduction

Photovoltaic devices based on organic materials are currently one of the most promising renewable and alternative energy sources available, because of their low cost, easy fabrication, and mechanical flexibility [1,2]. Two vital materials for general organic bulk heterojunction systems are poly(3-hexylthiophene) (P3HT) as the electron donor and [6,6]-pheny1-C61-butyric acid methyl ester (PCBM) as the electron acceptor, which have demonstrated the effective device performance [3,4]. In polymer photovoltaic systems, the simplest sandwich structure consists of a bulk heterojunction as the active layer, indium tin oxide (ITO) combined with a high conductive layer of poly(3,4-ethylenedioxythiophene):poly(styrenesulfonate) (PEDOT:PSS) as the anode, and aluminum (Al) as the cathode. It is well known that devices based on P3HT mixed with PCBM under a post-annealing process have enhanced performance compared to those under pre-annealing. This is a direct result of the enlarged interfacial roughness of the active layer, the chemical reaction at the interface of the active layer/cathode, and the formation of the Al–PCBM complex at the interface during the thermal annealing process [5–9]. The enlarged interfacial roughness of the active layer leads to the advantages of reducing the charge transport distance and creating more effective charge collection at the interfaces, as mentioned in most of the previous studies [10–12]. However, no study to date has examined the basic mechanism that leads to the morphology changes of the active layer. In this study, the formation of interfacial wrinkles around the cathode, which is related to the morphology changes of the active layer, is investigated. Systematic investigations are focused on providing a comprehensive explanation of the underlying mechanisms at work.

2. Experimental

The devices were fabricated on patterned ITO-coated glass substrates as the anode. The surface of the ITO substrate was modified by spin-coating conductive PEDOT:PSS with a thickness of approximately 40 nm and then baked at 120 °C for 60 min in ambient air. P3HT was blended with PCBM (at a 1:1 weight ratio) and dissolved in 1,2-dichlorobenzene. The active layer was thermally annealed at 150 °C for 10 min in a nitrogen-filled glove box before (pre-annealing) or after (post-annealing) the aluminum deposition. The cathode comprising a 100 nm Al layer was thermally evaporated on the polymer film, forming an active area of 0.06 cm^2 under a base pressure of 7.5×10^{-9} Pa.

The current density–voltage (J–V) characteristics of the devices were recorded under light illumination using a standard solar irradiation of 100 mW/cm^2 (AM1.5G) with a xenon lamp as the light source and a computer-controlled voltage–current Keithley 2400 Source Meter. To measure the surface of the active layer following the effect of capping the Al cathode under various fabrication processes, the Al electrode was removed with 1 M HCl solution for 10 min and rinsed with de-ionized water [11]. The topography and roughness of each

* Corresponding author. Tel.: +886 3 8634192; fax: +886 3 8634180.
E-mail address: meihsinchen@mail.ndhu.edu.tw (M.-H. Chen).

0040-6090/$ – see front matter © 2014 Elsevier B.V. All rights reserved.
http://dx.doi.org/10.1016/j.tsf.2014.01.038

surface were measured using atomic force microscopy (AFM) (Veeco Instruments, Caliber), and the AFM images were taken immediately after the samples were prepared. The nanoindentation experiments were measured with a Berkovich diamond indenter (TI950). The displacements into the surface were set within one tenth of the film thickness under contact loading rates of 0.7 μN/s and 0.2 μN/s for Al and organic thin films, respectively.

3. Results and discussion

Fig. 1(a) shows the performance of the devices with respect to current–voltage characteristics. Both pre-annealing and post-annealing processes were applied on the same device structure (ITO/PEDOT:PSS/P3HT:PCBM/Al). The device subject to post-annealing processes showed better performance, power conversion efficiency (PCE) of 3.02%, than that subject to pre-annealing processes (PCE = 1.81%), which agrees with previous studies [5]. In this study, it was observed that the cathode surfaces of the devices under the two types of annealing processes were noticeably different. Fig. 1(b) and (c) shows the optical microscopy images of the cathode surfaces on the devices after pre-annealing and post-annealing processes, respectively. The wrinkles are more prominent on the cathode surface of the devices subject to the post-annealing process. Thus, this study focuses on understanding the formation mechanisms of the wrinkles, which are anticipated to be influenced by the enlarged interfacial roughness of the active layer within the device using post-annealing processes.

During fabrication of the devices using pre-annealing processes, the as-cast P3HT:PCBM required thermal annealing at 150 °C for 10 min prior to the deposition of the Al cathode. For the fabrication of the devices using post-annealing processes, the as-cast P3HT:PCBM was deposited with the Al cathode and then was annealed at 150 °C for 10 min. As a result, wrinkles are formed more prominently on the cathode surface using the post-annealing process in comparison to using the pre-annealing process. The morphologies of each surface, which are related to the enlarged interfacial roughness of the active layer, under pre-annealing/post-annealing processes are further investigated with AFM to make systematic comparisons. The AFM images and the root mean square (rms) roughness obtained from each surface could then be compared to find out the underlying mechanisms leading to the change of morphology. Consequently, there are three types of morphologies shown in Fig. 2 and Fig. 3 for surfaces under pre-annealing and post-annealing processes, respectively. The three morphologies include the surface of the P3HT:PCBM before Al deposition, the surface of the Al cathode, and the surface of the P3HT:PCBM after removing the Al cathode.

Figs. 2(a) and 3(a) show the AFM images of an area of 10 μm × 10 μm and cross-section profiles for the surfaces of the active layer before Al deposition under pre-annealing/post-annealing processes, respectively. For the device using the pre-annealing process, the as-cast P3HT:PCBM had to be annealed at 150 °C for 10 min prior to cathode deposition, which was not applied to the devices using post-annealing processes. The values of the rms roughness of Figs. 2(a) and 3(a) are 8.7 nm and 13.5 nm, respectively. The slight morphology changes of the active layer with and without an annealing process applied can be examined through the glass transition temperature (T_g). In previous studies, the onset of the T_g of P3HT was observed at approximately 110 °C, and the T_g of PCBM was from 103 °C to 119 °C [6,13]. The annealing temperature of 150 °C of the active layer is greater than the T_g of the P3HT and PCBM materials. Therefore, the morphology of the active layer is lightly smoothed following thermal annealing above the T_g points because the molecules obtain enough energy and self-organize in the nanostructure.

The AFM image of the cathode surface (100 nm of Al) of the device subject to pre-annealing processes is shown in Fig. 2(b) with an rms

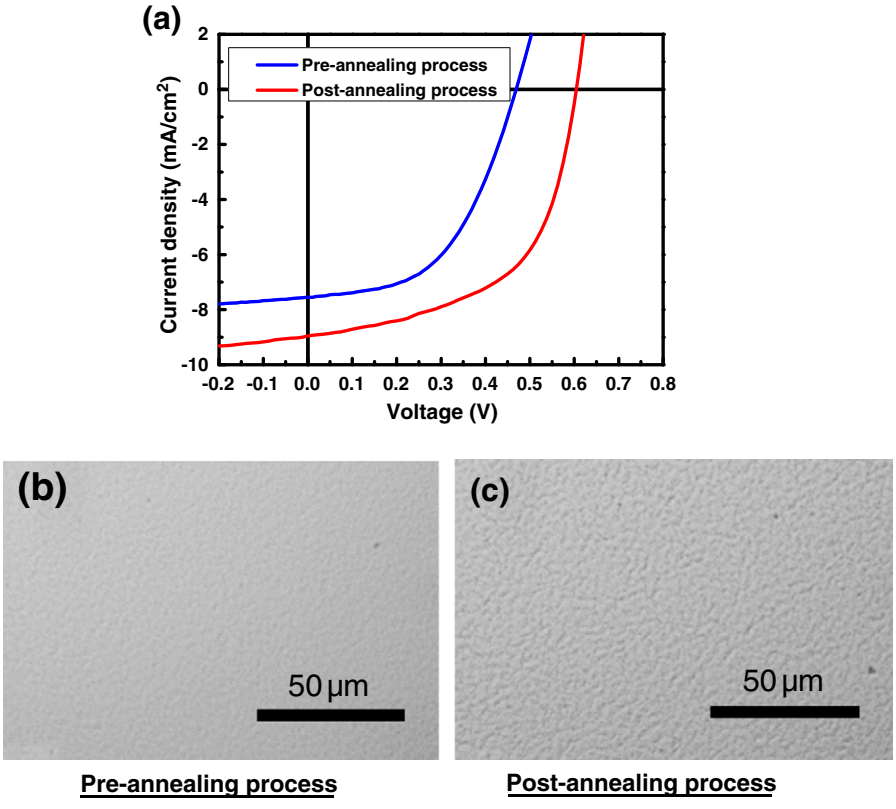

Fig. 1. (a) The current density–voltage (J–V) characteristics using pre-annealing/post-annealing processes of the polymer photovoltaics with the structures ITO/PEDOT:PSS/P3HT:PCBM/Al. (b) An optical microscopy image of the cathode surface on the device with pre-annealing processes. (c) The optical microscopy image of the cathode surface on the device with post-annealing processes.